appear as a contradiction, that below the crossing temperature of the Arrhenius curves (between around -25 and -30 °C) the Cope rearrangement-reorientation process is faster than the pure (3-fold) jump process.

In principle another dynamic process that preserves crystal order should also be considered, i.e., translational self-diffusion. Such a process occurs via molecular diffuse jumps between lattice sites, and for bullvalene we need to consider two situations: (i) When the jumps are between equivalent sites (see Figure 1), they will in general be accompanied by reorientation about the molecular C_3 axes, and the effect on the NMR spectrum will be identical to that for pure 3-fold jumps. (ii) If the diffusive jumps occur between different lattice sites, the process will also involve a change in orientation of the molecular symmetry axes. In the present work we only recorded spectra at magnetic field orientations where all crystal sites were equivalent and therefore only the 3-fold jump part of such diffuse jumps would be felt. We plan to extend our measurements to single crystals at general orientations of the magnetic field in order to determine whether such diffuse jumps occur on the NMR time scale. For now we can only set an upper limit to the self-diffusion constant by assuming that the 3-fold jumps are entirely due to diffusion. Using Einstein's diffusion equation $l^2 = 6Dt$ with l equal to an average lattice distance in bullvalene (~5.6 Å) and t of the order of the correlation time for the 3-fold jumps (~ 10^{-4} s at room temperature) we obtain $D < 5 \times 10^{-12}$ cm^2 s^{-1}. For comparison for adamantane, which has a similar molecular shape, $D \sim 10^{-21}$ cm^2 s^{-1} at room temperature.[18] It is therefore most likely that self-diffusion in bullvalene is too slow to affect the NMR line shape in our measurements, but only additional experiments can tell for sure.

It is interesting to compare our results for solid bullvalene with those of Miller and Yannoni[19] for the analogous process in semibullvalene. In this case the Cope rearrangement in solution is extremely fast[20] and freezes out (on the NMR time scale) only around -170 °C. In contrast, in solid semibullvalene no effect on the ^{13}C MAS-NMR line shape due to the Cope rearrangement was observed up to its melting temperature (-85 °C). Apparently in this case the solid packing energy and the nonglobular shape of the molecule prevents reorientation of the molecules and hence the bond shift from taking place. Yannoni and co-workers have also shown[21] that by annealing semibullvalene the bond isomerization becomes extremely fast, apparently due to introduction of disorder.

Acknowledgment. We thank Professor G. Schröder for a generous gift of a bullvalene sample from which the deuterated compound was prepared. We also thank Drs. T. Bernhard, M. Eisenstein, F. Frolow, and U. Haeberlen for numerous discussions concerning the crystal structure of bullvalene and its deuterium NMR spectrum. One of us (S.S.) thanks the Weizmann Institute of Science for a Rosie and Max Varon visiting professorship and the National Science Foundation for a grant, No. DMR-8718947. This work was supported by the Israel Academy of Sciences, Jerusalem.

Registry No. Bullvalene, 1005-51-2.

(18) Resing, H. A. *Mol. Cryst. Liq. Cryst.* **1969**, *9*, 101.

(19) Miller, R. D.; Yannoni, C. S. *J. Am. Chem. Soc.* **1980**, *102*, 7397.
(20) Cheng, A. K.; Anet, F. A. L.; Mioduski, J.; Meinwald, J. *J. Am. Chem. Soc.* **1974**, *96*, 2887.
(21) Macho, V.; Miller, R. D.; Yannoni, C. S. *J. Am. Chem. Soc.* **1983**, *105*, 3735.

Relationship between Amide Proton Chemical Shifts and Hydrogen Bonding in Amphipathic α-Helical Peptides

Nian E. Zhou, Bing-Yan Zhu, Brian D. Sykes, and Robert S. Hodges*

Contribution from the Department of Biochemistry and the Protein Engineering Network of Centres of Excellence, University of Alberta, Edmonton, Alberta, Canada T6G 2H7.
Received October 7, 1991

Abstract: The relationship between amide proton chemical shift and hydrogen bond length has been investigated for a designed amphipathic α-helical peptide (Ac-Glu-Leu-Glu-Lys-Leu-Leu-Lys-Glu-Leu-Glu-Lys-Leu-Leu-Lys-Glu-Leu-Glu-Lys-NH_2). Four important results were obtained. (1) The secondary chemical shifts ($\Delta\delta_{HN}$) changed periodically in a 3-4 repeat pattern along the peptide chain except for the first three residues at the N-terminal end of the peptide. The amide proton exhibits a large positive chemical shift in the center of the hydrophobic face and a large negative chemical shift in the center of the hydrophilic face. For the amide protons that are hydrogen-bonded between residues in the hydrophobic and hydrophilic faces, their chemical shifts are close to the random-coil values. (2) The $\Delta\delta_{HN}$ values at positions 9 and 13 are correlated with the decrease in the hydrophobicity of the side chain substituted at position 9 (Leu, Ala, and Gly). (3) The amplitude of $\Delta\delta_{HN}$ is dependent upon the amphipathicity of the peptide; that is, a peptide with a higher hydrophobic moment has a greater amplitude of $\Delta\delta_{HN}$. (4) The hydrogen-bond lengths calculated from amide chemical shifts are similar to those measured from computer-modeling experiments of a curved α-helix. These results indicate that the amide proton chemical shift is related to hydrogen-bond length and that a single-stranded amphipathic α-helix in solution is curved and this curved structure causes the upfield shifts of amide protons in the convex side and downfield shifts of amide protons in the concave side.

Introduction

It has long been recognized that ^{1}H-NMR chemical shifts in proteins are sensitive not only to the local electronic structure but also to shielding effects that result from the formation of secondary and tertiary structure upon protein folding.[1] The chemical shifts of amino acids in a protein are generally quite different from random-coil values. This sensitivity of chemical shifts to the secondary structure of proteins has been used to deduce structural information.[2-4] In particular, both theoretical calculations[5,6] and

(1) Wuthrich, K. *NMR of Proteins and Nucleic Acids*; Wiley: New York, 1986.

(2) Pastore, A.; Sandek, V. *J. Magn. Reson.* **1990**, *90*, 165-176.
(3) Szilagyi, L.; Jardetzky, O. *J. Magn. Reson.* **1989**, *83*, 441-449.
(4) Wishart, D. S.; Sykes, B. D.; Richards, F. M. *J. Mol. Biol.* **1991**, *222*, 311-333.

0002-7863/92/1514-4320$03.00/0

statistical analysis[2-4] have shown that the α-CH proton chemical shift of an amino acid residue in peptides and proteins is shifted upfield (lower chemical shift values) in α-helices and downfield (higher chemical shift values) in β-strands in comparison to those in the random-coil structure. However, the relationship between the amide proton chemical shifts and the secondary structure is still not well understood.[2,7] Statistical analysis of protein secondary structure and the amide proton chemical shifts indicated that, on average, the amide protons resonate to upfield in α-helices and downfield in β-strands.[4,8] Recently, Kuntz et al.[7] observed that the amide protons in many α-helices show a 3–4 repeat periodicity in chemical shifts and postulated that this periodic change is caused by the curvature of protein and peptide α-helical structures in solution.

Perhaps the best example of curved α-helices in proteins is the two-stranded α-helical coiled-coil (GCN4 leucine zipper). The X-ray crystal structure at 1.8-Å resolution shows that the individual α-helices are smoothly bent and the curvature is associated with shorter main-chain hydrogen bonds in the interface compared to the outside of the helices.[9] In addition, the NMR data obtained by Oas et al.[10] for this coiled-coil and analyzed by Kuntz et al.[7] showed this regular periodicity of the amide chemical shifts. The question to be addressed is whether the α-helix curvature is a result of the interchain interactions between the α-helices or whether it is an inherent property of the individual amphipathic α-helix. Therefore, we have designed de novo amphipathic α-helical peptides and studied them by CD and NMR spectroscopy in solution as noninteracting α-helices by maintaining the peptides as single-stranded α-helices. The relationship between amide chemical shift and hydrogen-bond length was investigated. We have demonstrated that the amide proton chemical shift in single-stranded amphipathic α-helical peptides is closely related to the hydrogen-bond length in the α-helix and consequently to the curvature of an amphipathic α-helix. In general, the amide proton in the center of a hydrophobic face (i.e., the NH of a hydrophobic residue that is hydrogen-bonded with the carbonyl of another hydrophobic residue) exhibits a large positive chemical shift compared to the random-coil value. In contrast, the amide proton in the center of a hydrophilic face (i.e., the NH of a hydrophilic residue that is hydrogen-bonded with the carbonyl of another hydrophilic residue) exhibits a large negative chemical shift compared to the random-coil value. For the NH protons that are hydrogen-bonded between residues in the hydrophobic and hydrophilic faces, their chemical shift values are close to that of the random-coil value.

Materials and Methods

Peptide Synthesis and Characterization. All peptides were synthesized by the solid-phase technique starting with copoly(styrene, 1% divinylbenzene)–benzhydrylamine hydrochloride resin and using an Applied Biosystems Model 430A peptide synthesizer as described previously.[11] The peptide was cleaved from the resin by reaction with hydrogen fluoride (20 mL/g of resin) containing 10% anisole and 2% 1,2-ethanedithiol for 1 h at −5 °C. The crude peptides were purified by reversed-phase HPLC on a Synchropak RP-P semipreparative C18 column (250 × 10 mm i.d., 6.5-μm particle size, 300-Å pore size) (Synchrom, Lafayette, IN) with a linear AB gradient (ranging from 0.2% to 1.0% B/min, depending on the peptide) at a flow rate of 2 mL/min, where solvent A was 0.05% aqueous trifluoroacetic acid (TFA) and solvent B was 0.05% TFA in acetonitrile. Peptide purity was verified by analytical reversed-phase HPLC and amino acid analysis. Amino acid analysis was performed on a Beckman Model 6300 amino acid analyzer (Beckman Instruments Inc., Fullerton, CA). The correct primary ion molecular weights were confirmed by time of flight mass spectroscopy on a BIOI-ON-20 Nordic (Uppsala, Sweden).

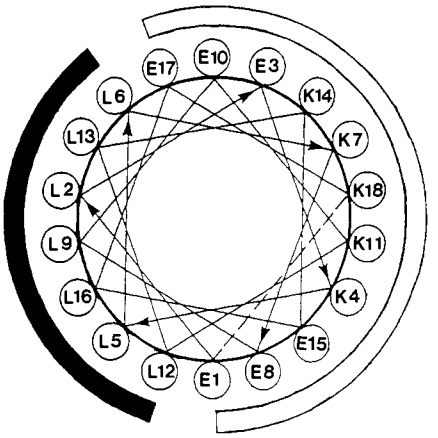

Figure 1. Amino acid sequence of the designed amphipathic α-helical peptide LL9 represented as a helical wheel. Since the α-helix has 3.6 residues per turn, adjacent side chains in the sequence are separated by 100° of arc on the wheel. The hydrophobic and hydrophilic faces are observed on opposing sides of the helix as indicated by the solid and open bars, respectively.

Circular Dichroism (CD) Experiments. Circular dichroism spectra were recorded at 20 °C on a Jasco J-500C spectropolarimeter (Jasco, Easton, MD) attached to a Jasco DP-500N data processor and a Lauda (Model RMS) water bath (Brinkman Instruments, Rexdale, Ontario, Canada) used to control the temperature of the cell. The instrument was routinely calibrated with an aqueous solution of recrystallized *d*-10-camphorsulfonic acid. Ellipticity is reported as mean residue molar ellipticity [θ]. Peptide concentrations were determined by amino acid analysis.

^{1}H-NMR Experiments. Samples for 2D-NMR experiments were prepared as approximately 5 mM peptide solutions in a 1:1 mixture of trifluoroethanol-d_3 (TFE-d_3) (Cambridge Isotopes Laboratory) and H_2O containing 0.1 M KCl, 50 mM potassium phosphate buffer. The pH of the sample was adjusted to 5.2 with dilute HCl and KOH. pH meter readings were measured at room temperature and were not corrected.

All NMR spectra were obtained on a Varian VXR-500 NMR spectrometer with an operating frequency of 500 MHz for protons. Chemical shifts were referenced to the trimethylsilyl resonance of 2,2-dimethyl-2-silapentane-5-sulfonate (DSS) at 0.00 ppm. Spectra were normally taken at 25 °C. All 2D spectra (NOESY,[12] DQF-COSY,[13] and HOHAHA[14]) were obtained in the phase-sensitive detection mode by using standard pulse sequences. Spectra were acquired with 2048 complex points in t_2 and 256–512 complex FIDs in t_1 with 24–64 transients for each FID. The carrier was centered on the H_2O resonance, and the spectral width was 6000 Hz in both dimensions. HOHAHA spectra were collected with mixing times of 30 ms. NOESY spectra were collected with mixing times of 400 ms. The amide proton exchange rate was monitored by one-dimensional spectra at 25 °C in a 1:1 mixture of TFE-d_3 and D_2O containing 0.1 M KCl, 50 mM potassium phosphate, pH 5.2 solution.

Computer Modeling. The α-helical model of the peptide was built on a silicon Graphics Personal Iris with the Insight II and Discover programs (Biosym Technologies Inc., San Diego, CA).[15]

Results and Discussion

α-Helices in globular proteins are usually amphiphathic to provide hydrophobic interactions with the hydrophobic core that stabilizes the tertiary structure of the folded protein. We have designed and synthesized an 18-residue peptide with a high potential to form an amphipathic α-helical structure. The peptide amino acid sequence is Ac-Glu-Leu-Glu-Lys-Leu-Leu-Lys-Glu-Leu-Glu-Lys-Leu-Leu-Lys-Glu-Leu-Glu-Lys-NH_2. In Figure 1, the amino acid sequence of the model peptide is viewed as an axial projection of the α-helix in a helical wheel presentation. The hydrophobic amino acid residues (leucine) and hydrophilic residues

(5) Clayden, N. J.; Williams, R. J. P. *J. Magn. Reson.* **1982**, *49*, 393–396.
(6) Dalgarno, D. C.; Levine, B. A.; Williams, R. J. P. *Biosci. Rep.* **1983**, *3*, 443–452.
(7) Kuntz, I. D.; Kosen, P. A.; Craig, E. C. *J. Am. Chem. Soc.* **1991**, *113*, 1406–1408.
(8) Williamson, M. P. *Biopolymers* **1990**, *29*, 1423–1431.
(9) O'Shea, E. K.; Klemm, J. D.; Kim, P. S.; Alber, T. *Science* **1991**, *254*, 539–544.
(10) Oas, T. G.; McIntosh, L. P.; O'Shea, E. K.; Dahlquist, F. W.; Kim, P. S. *Biochemistry* **1990**, *29*, 2891–2894.
(11) Hodges, R. S.; Semchuk, P. D.; Taneja, A. K.; Kay, C. M.; Parker, J. M. R.; Mant, C. T. *Pept. Res.* **1988**, *1*, 19–30.
(12) Kumar, A.; Ernst, R. R.; Wuthrich, K. *Biochem. Biophys. Res. Commun.* **1980**, *95*, 1–6.
(13) Rance, M.; Sorensen, M.; Bodenhausen, G.; Wagner, G.; Ernst, R. R.; Wuthrich, K. *Biochem. Biophys. Res. Commun.* **1983**, *117*, 479–485.
(14) Davis, D. G.; Bax, A. *J. Am. Chem. Soc.* **1985**, *107*, 7197–7198.
(15) Mackay, D. H. J.; Cross, A. J.; Hagler, A. T. In *Prediction of Protein Structure and the Principles of Protein Conformation*; Fasman, G. D. Ed.; Plenum Press: New York, 1980; pp 317–358.

Table I. Proton Chemical Shifts of Peptide LL9[a]

residue	NH	$C_\alpha H$	$C_\beta H$, $C_\beta H$	$C_\gamma H$, $C_\gamma H$	$C_\delta H$, $C_\delta H$	$C_\epsilon H$, $C_\epsilon H$	methyl
$-COCH_3$							2.16
Glu-1	8.32	4.23	2.04, 2.04	2.42, 2.15			
Leu-2	8.07	4.17	1.73, 1.73	1.64			0.91
Glu-3	8.28	3.93	2.07, 2.07	2.15, 2.38			
Lys-4	7.56	4.02	1.99, 1.99	1.60, 1.47	1.75, 1.75	3.02, 3.02	
Leu-5	7.80	4.16	1.78, 1.94	1.94			0.91
Leu-6	8.48	4.11	1.93, 1.93	1.58			0.89
Lys-7	8.01	4.16	2.10, 2.10	1.95, 1.52	1.75, 1.75	3.03, 3.03	
Glu-8	8.03	4.20	2.21, 2.21	2.34, 2.52			
Leu-9	8.62	4.18	1.77, 1.77	1.85			0.96
Glu-10	8.36	3.92	2.28, 2.28	2.54, 2.20			
Lys-11	7.64	3.99	2.05, 2.05	1.48, 1.70	1.78, 1.78	3.02, 3.02	
Leu-12	7.98	4.17	2.00, 1.78	1.78			0.91
Leu-13	8.69	4.06	1.93, 1.93	1.54			0.90
Lys-14	8.08	4.09	2.07, 2.07	1.93, 1.54	1.72, 1.72	3.03, 3.03	
Glu-15	7.98	4.17	2.22, 2.22	2.36, 2.50			
Leu-16	8.50	4.16	2.00, 2.00	1.58			0.91
Glu-17	8.11	4.12	2.21, 2.21	2.60, 2.44			
Lys-18	7.64	4.19	1.99, 1.99	1.70, 1.57	1.77, 1.77	3.02, 3.02	
NH_2-19	7.25						
	6.96						

[a] In 50% TFE-d_3 and 50% H_2O containing 0.1 M KCl, 50 mM phosphate, pH 5.2, at 25 °C.

(glutamic acid and lysine) are separated on two sides of the α-helix to form an amphipathic α-helix. The model peptide is denoted as LL9 where the first L refers to the peptide with seven leucines in the hydrophobic face including position 9 (L9). When the leucine residue at position 9 is substituted by an alanine or glycine, the peptide analogue is denoted as LA9 or LG9, respectively. When all seven leucine residues in the hydrophobic face are replaced by seven alanines, the peptide analogue is denoted as AA9.

In the design of this model peptide, leucine, glutamic acid, and lysine were selected specifically because of their highly intrinsic helical propensities,[16-18] leucine as an apolar aliphatic residue and glutamic acid and lysine as charged residues. Previous studies in our laboratory[19-22] and others[23-26] have demonstrated that hydrophobic interactions can play a dominant role in secondary-structure formation and contribute in a major way to the stability of α-helices in aqueous solution. The amino acid sequences of α-helices tend to have a strong periodic distribution of hydrophobic amino acids along the chain with a 3–4 residue repeat.[25,27,28] Hydrophobic residues tend to cluster into the solvent-inaccessible interiors of globular proteins, while hydrophilic residues tend to project outward and are more solvated. The glutamate/lysine ion pairs located in i and $i + 3$ or i and $i + 4$ positions along the sequence could provide additional stability to the α-helical structure by side-chain electrostatic interactions.[29,30]

Helicity of the Model Peptide. The α-helicity of the model peptide was determined by CD experiments. The CD spectra were measured in 0.1 M KCl, 50 mM potassium phosphate buffer (pH 5.2) containing trifluoroethanol (TFE), 1:1 (v/v), a solvent that induced helicity in single-chain potentially α-helical peptides.[31,32] Previous studies in our laboratory[33,34] have shown that 50% TFE disrupts the quaternary structure of α-helical coiled-coils, producing single-stranded α-helices; i.e., TFE is a denaturant of tertiary and quaternary structure stabilized by hydrophobic in-

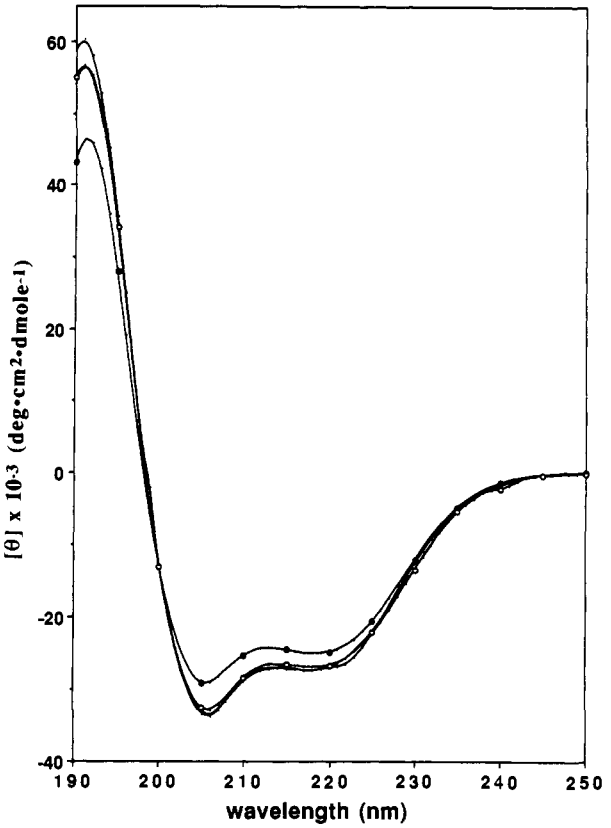

Figure 2. Circular dichroism spectra of α-helical peptides AA9 (●) and LA9, LG9, LL9 (○) in a 1:1 mixture (v/v) of TFE and buffer containing 0.1 M KCl, 50 mM potassium phosphate, pH 5.2. The temperature was 20 °C for ellipticity measurements.

(16) Chou, P. Y.; Fasman, G. D. *Annu. Rev. Biochem.* **1978**, *47*, 251–276.
(17) Sueki, M.; Lee, S.; Powers, S. P.; Denton, J. B.; Konishi, Y.; Scheraga, H. A. *Macromolecules* **1984**, *17*, 148–155.
(18) Scheraga, H. A. *Pure Appl. Chem.* **1978**, *50*, 315–324.
(19) Hodges, R. S.; Zhou, N. E.; Kay, C. M.; Semchuk, P. D. *Pept. Res.* **1990**, *3*, 123–137.
(20) Hodges, R. S.; Saund, A. K.; Chong, P. C. S.; St.-Pierre, S. A.; Reid, R. E. *J. Biol. Chem.* **1981**, *256*, 1214–1224.
(21) Lau, S. Y. M.; Taneja, A. K.; Hodges, R. S. *J. Biol. Chem.* **1984**, *259*, 13253–13261.
(22) Zhou, N. E.; Zhu, B.-Y.; Kay, C. M.; Hodges, R. S. *Biopolymers*, in press.
(23) DeGrado, W. F.; Lear, J. D. *J. Am. Chem. Soc.* **1985**, *107*, 7684–7689.
(24) DeGrado, W. F.; Wasserman, Z. R.; Lear, J. D. *Science* **1989**, 622–628.
(25) Eisenberg, D.; Weiss, R. M.; Terwilliger, T. C. *Proc. Natl. Acad. U.S.A.* **1984**, *81*, 140–144.
(26) Kanehisa, M. I.; Tsang, T. Y. *Biopolymers* **1980**, *19*, 1617–1628.
(27) Torgerson, R. R.; Lew, R. A.; Reges, V. E.; Hardy, L.; Humphreys, R. E. *J. Biol. Chem.* **1991**, *266*, 5521–5524.
(28) Talbot, J. A.; Hodges, R. S. *Acc. Chem. Res.* **1982**, *15*, 224–230.
(29) Marqusee, S.; Baldwin, R. L. *Proc. Natl. Acad. Sci. U.S.A.* **1987**, *84*, 8898–8902.
(30) Merutka, G.; Stellwagen, E. *Biochemistry* **1991**, *30*, 1591–1594.
(31) Nelson, J. W.; Kallenbach, N. R. *Proteins* **1986**, *1*, 211–217.
(32) Nelson, J. W.; Kallenbach, N. R. *Biochemistry* **1989**, *28*, 5256–5261.
(33) Lau, S. Y. M.; Taneja, A. K.; Hodges, R. S. *J. Chromatogr.* **1984**, *317*, 129–140.
(34) Zhou, N. E.; Mant, C. T.; Hodges, R. S. *Pept. Res.* **1990**, *3*, 8–20.

Figure 3. Summary of the sequential and medium-range NOEs observed for peptide LL9. Solid lines indicate unambiguous NOEs, dashed lines indicate ambiguous NOEs due to spectral overlap, and widths of the lines indicate the intensities of the NOEs.

teractions. Due to the high amphipathicity of the designed peptides, they could easily aggregate in aqueous solution through the intermolecular hydrophobic interactions. Size-exclusion chromatographic results have shown that these peptides are monomeric when the TFE concentration in solution is higher than 25% (v/v).[35]

All of the CD spectra of the peptides (Figure 2) showed two minimum absorption peaks, one near 220 nm ($n\pi^*$ transition) and another at 206 nm ($\pi\pi^*$ transition). The helical content of each peptide was calculated from the value of the mean residue molar ellipticity at 220 nm ($[\theta]_{220}$). The value of −31 060 deg·cm^2/dmol was used as an estimate of a 100% α-helical 18-residue peptide.[36] The observed ellipticities of −26 640, −26 970, −26 770, and −24 810 deg·cm^2/dmol in 50% TFE (pH 5.2) yield estimates of 86%, 87%, 86%, and 80% α-helix for peptides LL9, LA9, LG9, and AA9, respectively.

α-Helical Structure of the Peptide Determined by ^{1}H-NMR Spectroscopy. Though CD spectroscopy can provide an estimate of the α-helical content of a peptide, analysis of peptide structure by NMR techniques can determine precisely the location and extent of helical structure in the peptide. The complete assignments of all amide proton, α-CH proton, and other proton chemical shifts were achieved by using the standard sequential assignment[1] and main-chain-directed approach[37] on the basis of 2D-NMR spectra (DQF-COSY, HOHAHA, and NOESY). The chemical shifts of peptide LL9 are listed in Table I. NOE connectivities observed between protons of neighboring and nonneighboring amino acid residues indicated that the peptide LL9 is helical in solution. In an ideal α-helix, $d_{NN(i,i+1)}$ and $d_{\alpha N(i,i+1)}$ distances are 2.8 and 3.5 Å, respectively. These distances are 4.3 and 2.2 Å, respectively, in an extended chain.[38] Therefore, the $d_{NN(i,i+1)}$ cross-peak should be much more intense than the $d_{\alpha N(i,i+1)}$ cross-peak in an α-helical structure.[39] Strong sequential connectivities $d_{NN(i,i+1)}$ and weaker sequential connectivities $d_{\alpha N(i,i+1)}$ were observed between all amino acids except residue Glu-1, where the $d_{\alpha N(1,2)}$ cross-peak is stronger than that of $d_{NN(1,2)}$ (Figure 3). A more stringent criterion for helical structure is the presence of medium-range $d_{\alpha\beta(i,i+3)}$ and $d_{\alpha N(i,i+3)}$ NOE connectivities.[1,40] Such $i, i+3$ NOEs define a helical conformation with a very high degree of reliability when they occur in sequential series. Most of the medium-range NOE connectivities, which characterize α-helical structures ($d_{\alpha N(i,i+3)}$ and $d_{\alpha\beta(i,i+3)}$), were observed for peptide LL9 (Figure 3).

It is well-known that the α-proton chemical shifts of amino acid residues tend to upfield values (relative to the random-coil value) in α-helical structures.[2-4] A plot of the difference between the chemical shifts of the α-protons and those in a random coil of the same sequence vs the position along the peptide sequence is a simple and effective way to relate chemical shifts to features of secondary structure.[2,41] Figure 4 shows such a plot for peptide

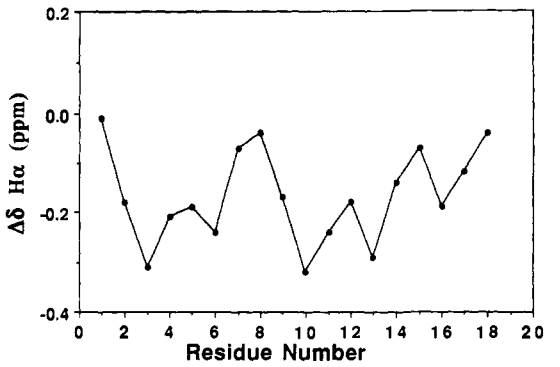

Figure 4. Plot of the difference between the chemical shifts of the α-proton of a particular residue in the peptide and that in a random-coil conformation ($\Delta\delta_{H_\alpha}$) vs the position along the sequence for peptide LL9. $\Delta\delta_{H_\alpha} = \delta_{H_\alpha}(\text{obsd}) - \delta_{H_\alpha}(\text{random coil})$. The random-coil values were taken from ref 4.

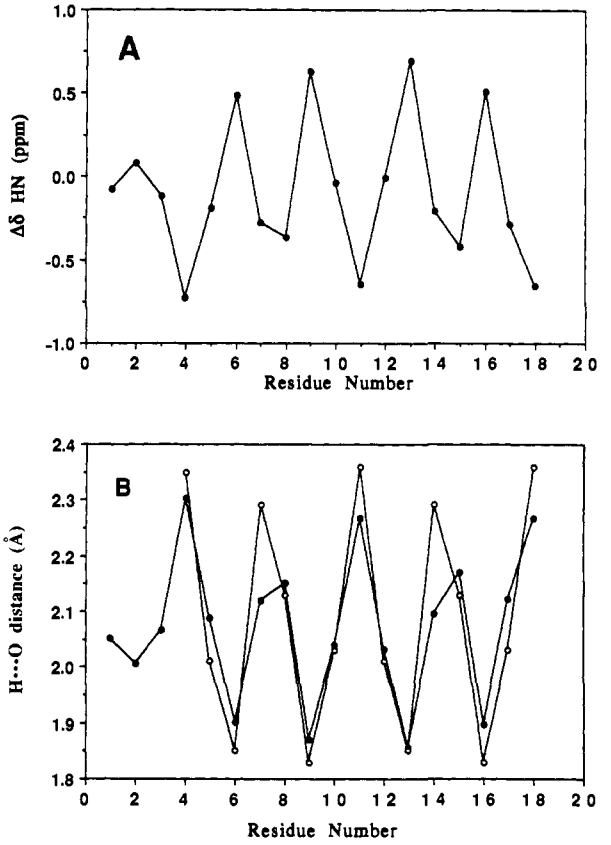

Figure 5. (A) Plot of the difference between the chemical shifts of the amide proton of a particular residue in the peptide and of that in a random-coil conformation ($\Delta\delta_{HN}$) vs the position along the sequence for peptide LL9. $\Delta\delta_{HN} = \delta_{HN}(\text{obsd}) - \delta_{HN}(\text{random coil})$. The random coil values were taken from ref 4. (B) Comparison between hydrogen-bond lengths (the distance from the carbonyl oxygen to the amide proton) obtained from the amide chemical shifts (●) and those measured from the computer-modeling structure of a curved α-helix (○). The hydrogen-bond length obtained from the amide chemical shifts was calculated according to the equation $\Delta\delta_{HN} = 19.2d^{-3} - 2.3$, where $\Delta\delta_{HN}$ is the chemical shift difference between the amide proton and the random-coil proton in ppm and d is the hydrogen-bond length in angstroms.[42,43] See text for details.

(35) Zhou, N. E. Unpublished results.
(36) Chen, Y.-H.; Yang, T. J.; Chau, K. H. *Biochemistry* **1974**, *13*, 3350–3359.
(37) Englander, S. W.; Wand, A. J. *Biochemistry* **1987**, *26*, 5953–5958.
(38) Billeter, M.; Brown, W.; Wuthrich, K. D. *J. Mol. Biol.* **1982**, *155*, 311–320.
(39) Bradley, E. K.; Thomason, J. F.; Cohen, F. E.; Kosen, P. A.; Kuntz, I. D. *J. Mol. Biol.* **1990**, *215*, 607–622.
(40) Wuthrich, K.; Billeter, M.; Braun, W. *J. Mol. Biol.* **1984**, *180*, 715–740.
(41) Pastore, A.; DeFrancesco, R.; Barbato, G.; Morelli, M. A. C.; Motta, A.; Cortese, R. *Biochemistry* **1991**, *30*, 148–153.

LL9 (random-coil values of Wishart et al.[4]). The negative $\Delta\delta$ values from residues Lys-2 to Glu-17 suggested that the peptide is α-helical through the majority of the sequence. The NOE connectivities and α-proton chemical shifts described above provide independent and direct evidence that the α-helical structure extends along the entire peptide chain (LL9) except the terminal residues. Similar results were also obtained for peptides LA9 and LG9. These results are in good agreement with the CD data.

Correlation between Amide Proton Chemical Shifts and Hydrogen Bonds in an Amphipathic α-Helical Peptide. Figure 5A shows a plot of the difference between the chemical shifts of the amide protons and those in a random coil of the same sequence ($\Delta\delta$ = δ(obsd) - δ(random coil); random-coil values from ref 4) vs the amino acid position for peptide LL9. The $\Delta\delta$ values instead of absolute chemical shift values were used in the plot, in order to rule out differences in chemical shifts of individual amino acid residues. From Figure 5A, it is clearly seen that the $\Delta\delta$ value is changed periodically along the peptide chain with a 3–4 repeat pattern, four maximum positive $\Delta\delta$ values at positions 6, 9, 13, and 16 and five maximum negative $\Delta\delta$ values at positions 4, 8, 11, 15, and 18. These results are consistent with the observation by Kuntz et al.[7] that the amide protons in many α-helices showed a 3–4 repeat periodicity in chemical shifts. On average (in consideration of all 20 naturally occurring amino acids), resonances of amide protons in α-helical structures are upfield relative to random-coil values. But not all of the amide protons in α-helices shift upfield. Even for the same amino acid in the same secondary structure, i.e., an α-helix, some amide protons shift downfield and some are close to random-coil values. For example, of the seven amide proton resonances of the leucine residues on the nonpolar face of the amphipathic α-helix, three are close to random-coil values at positions Leu-2, Leu-5, and Leu-12 and four shift significantly downfield at positions Leu-6, Leu-9, Leu-13, and Leu-16 (Figure 5A). These results indicate that the amide proton chemical shift is dependent not only on secondary structure but also on the location of the amino acid residue in the α-helix. All the amide protons in the center of the hydrophobic face shift downfield (Leu-6, Leu-9, Leu-13, and Leu-16), all the amide protons in the center of the hydrophilic face shift upfield (Lys-4, Lys-11, and Lys-18), and all the amide protons between the hydrophobic and hydrophilic faces show intermediate secondary chemical shifts ($\Delta\delta$) (Figure 5A).

The observation of amide chemical shift variation can be explained by the change of the hydrogen-bond length in the amphipathic α-helix. In an α-helical structure, the carbonyl oxygen at position i forms a hydrogen bond with the HN of an amino acid residue at position $i + 4$. The amide protons in the first three residues at the N-terminal end of the peptide were not involved in intramolecular hydrogen bonds. As shown in Figure 5A, the chemical shifts of the first three amide protons did not change significantly and were very close to the random-coil values (within 0.1 ppm). According to the relationship between the secondary chemical shift ($\Delta\delta$) of the amide proton and the distance of the amide proton to the carbonyl oxygen atom, the hydrogen-bond distances were calculated.[42,43] The positive secondary chemical shifts are correlated with the shorter hydrogen bonds, and the negative shifts, with the longer hydrogen bonds. The hydrogen bonds are shorter in the center of the hydrophobic face (Leu-6, Leu-9, Leu-13, and Leu-16) and longer in the center of the hydrophilic face (Lys-4, Lys-11, and Lys-18). The hydrogen bonds between the hydrophobic and hydrophilic faces are of intermediate lengths. These results are in good agreement with X-ray structures of many amphipathic α-helices in proteins. The survey of α-helices in proteins indicated that most α-helices are curved.[44] Amphipathic α-helices are not linear, and the α-helix axis is distorted to a curvature structure with the hydrophobic face being concave and the hydrophilic face being convex. The hydrogen bonds in the hydrophobic face are shorter and more linear than those in the hydrophilic face. The net effect of the distortions is to cause the residues on the two sides of a helix to have different main-chain torsion angles; those on the hydrophobic side have (Φ_{i+1}, Ψ_i) = (−59°, −44°), and those on the hydrophilic side have (Φ_{i+1}, Ψ_i) = (−66°, −41°).[44,45] A computer model of peptide LL9 was built on the basis of the general torsion (Φ, Ψ) angles for the curved α-helix. All i residues whose carbonyl is hydrogen-bonded to an amide of a hydrophobic residue were assigned (Ψ_i, Φ_{i+1}) = (−44°, −59°), whereas (−41°, −66°) was used for the remainder of the torsion angles (Ψ, Φ). Figure 5B shows a comparison between hydrogen-bond lengths (the distance from the carbonyl oxygen to the amide proton) obtained from amide chemical shifts and those measured from the computer-modeling structure of a curved α-helix. The similarity between hydrogen-bond lengths obtained from amide chemical shifts and those measured from the computer-modeling structure of the curved α-helix (Figure 5B) pro-

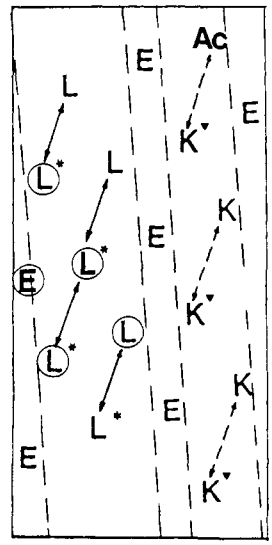

Figure 6. Sequence of peptide LL9 plotted as an α-helical net. The radius of the α-helix is taken as 2.5 Å with 3.6 residues per turn, a residue translation of 1.5 Å, and thus, a pitch of 5.4 Å. Solid arrows denote hydrogen bonds in the hydrophobic face, and dashed arrows denote hydrogen bonds in the hydrophilic face. Stars (*) denote the hydrophobic residues in the hydrophobic face whose amide protons are hydrogen-bonded to the carbonyl of another hydrophobic residue, resulting in significant positive $\Delta\delta_{HN}$ values. Closed trigons (▼) denote the hydrophilic residues in the hydrophilic face whose amide protons are hydrogen-bonded to the carbonyl of another hydrophilic residue, resulting in significant negative $\Delta\delta_{HN}$ values. The circles denote the amide protons of residues with slow deuterium-exchange rates (intensity loss is less than 80% after 12 h).

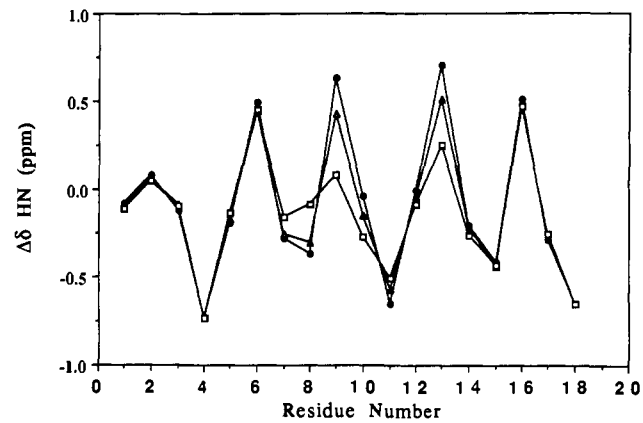

Figure 7. Plot of $\Delta\delta_{HN}$ (defined in panel A of Figure 5) vs residue number for peptides LL9 (●), LA9 (△), and LG9 (□).

(42) Wagner, G.; Pardi, A.; Wuthrich, K. *J. Am. Chem. Soc.* **1983**, *105*, 5948–5949.
(43) Pardi, A.; Wagner, G.; Wuthrich, K. *Eur. J. Biochem.* **1983**, *137*, 445–454.
(44) Barlow, D. J.; Thornton, J. M. *J. Mol. Biol.* **1988**, *201*, 601–619.
(45) Blundell, T.; Barlow, D.; Borkakoti, N.; Thornton, J. *Nature* **1983**, *206*, 281–283.

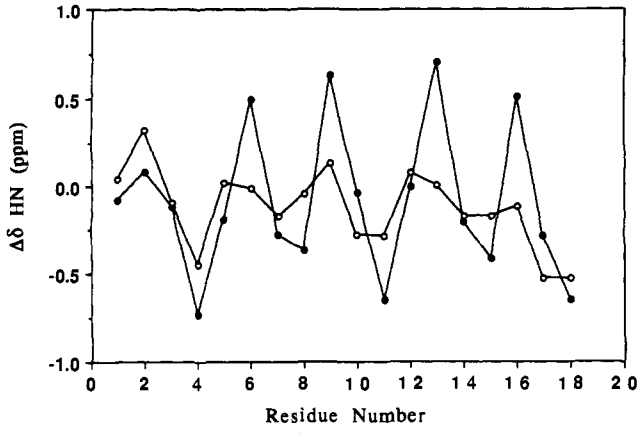

Figure 8. Comparison of $\Delta\delta_{HN}$ (defined in panel A of Figure 5) between peptides LL9 (●) and AA9 (○).

vided indirect evidence that the change of amide chemical shifts is related to the hydrogen-bond length and the amphipathic α-helix is curved in solution. A helical net (Figure 6) was used to illustrate these distortions for peptide LL9.

The effect of hydrogen-bond length on the HN chemical shifts is further supported by the results in Figure 7. Figure 7 shows the relationship between secondary chemical shifts ($\Delta\delta_{HN}$) and amino acid position for the two peptides where Ala and Gly were substituted for Leu at position 9 compared to the case of native peptide. As shown, the secondary chemical shifts for residues 1–6 and 14–18 are not changed among these peptide analogues. Interestingly, the secondary chemical shifts at positions 9 and 13 are correlated with the decrease in the hydrophobicity of the side chain substituted at position 9. We postulate that the Leu side chain at position 9 can protect its own hydrogen bond with the Leu-5 carbonyl. When Ala or Gly is substituted for Leu, there is a large decrease in hydrophobicity, which lengthens the hydrogen bond between the Ala or Gly amide proton and the carbonyl at Leu-5. In the case of the HN proton at position 13, it is hydrogen-bonded to the carbonyl oxygen at position 9. Similarly, when Ala or Gly was substituted for Leu at position 9, the hydrophobicity of the small side chain of Ala or Gly could not protect the hydrogen bond effectively, resulting in a longer hydrogen bond.

Effect of Amphipathicity of the α-Helical Peptide on the Amplitude of Secondary Amide Chemical Shift (Δδ). Blundell et al.[45] have generated, using X-ray crystallographic data and computer graphics, a series of helices with different amphipathic characters and found that the degree of curvature depends upon the extent of peptide amphipathicity; that is, peptides with higher hydrophobic moments have higher curvature. If the amphipathic α-helix in solution is also curved and this curved structure causes the upfield shifts of the amide protons in the convex side and downfield shifts of the amide protons in the concave side (as noted above), the amplitude of amide secondary chemical shift ($\Delta\delta_{HN}$) should be expected to depend upon the amphipathicity of the peptide. Figure 8 compares the secondary chemical shifts ($\Delta\delta_{HN}$) of the amide protons of peptides LL9 and AA9. The amplitude of Δδ of the amide protons is much smaller in peptide AA9 than in peptide LL9, as expected. The greater the hydrophobicity on the nonpolar face, the more the curvature. Both of the peptides LL9 and AA9 are highly α-helical, as demonstrated by CD and 2D-NMR spectroscopy, while the former is more amphipathic than the latter. Eisenberg's mean hydrophobic moment,[46,47] a numerical method, was used to express the helical amphipathicity of peptides. This method consists of the vector sum of the hydrophobicity values of the amino acids, taking into account their periodic orientation in the α-helix, i.e., one residue every 100° or 3.6 residues in a turn. The values of the mean helical hydrophobic moments are 0.73 for peptide LL9 and 0.59 for AA9. In addition, the plot of secondary chemical shift (Δδ) of the amide proton vs amino acid sequence for peptide AA9 (Figure 8) does not show 3–4 repeat periodicity as does that for peptide LL9, and the amide chemical shifts of peptide AA9 at positions 6, 9, 13, and 16 are decreased (compared to those in peptide LL9) and close to random-coil values. Comparison of amide chemical shifts between peptides LL9 and AA9 indicates that the changes of amide chemical shifts arise from distortions of hydrogen bonds in the α-helix rather than from the α-helical structure itself.

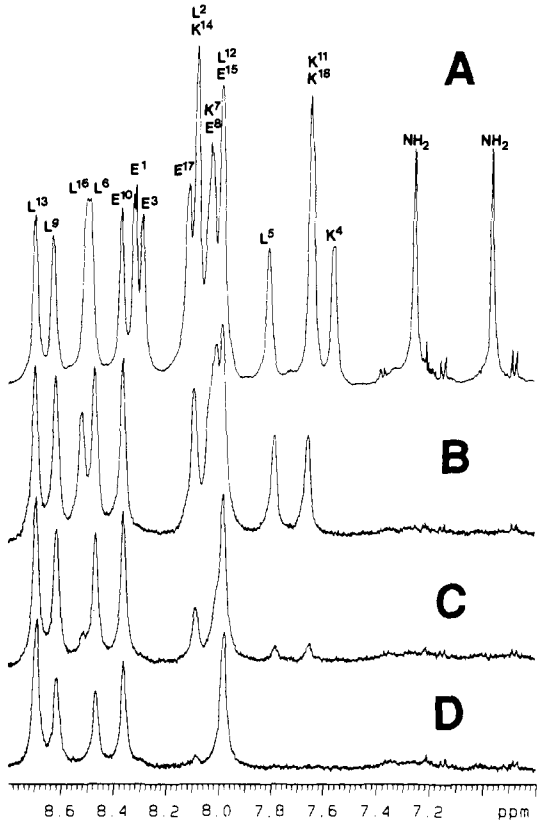

Figure 9. One-dimensional spectra of the amide resonances of peptide LL9 as a function of time after dissolving the peptide in 50% TFE-d_3 and 50% D_2O containing 0.1 M KCl, 50 mM phosphate, pH 5.2. Spectrum A is for the sample in 50% TFE-d_3 and 50% H_2O containing 0.1 M KCl, 50 mM phosphate, pH 5.2, and is used to represent the spectrum at time 0. The spectra were obtained at 25 °C with a 6000-Hz spectral width, 3-s acquisition time, 128 acquisitions, and a two-recycle delay, at 1 h (B), 5 h (C) and 12 h (D) after dissolving the sample in TFE-d_3/D_2O.

Amide Exchange Rate. An analysis of amide proton exchange rates can yield useful information regarding the hydrogen-bond stability and the accessibility of solvent molecules to the α-helical backbone in different regions of a peptide.[48,49] The amide hydrogen–deuterium exchange rates were obtained by monitoring the disappearance of the amide proton resonances as a function of time after redissolving the sample, which had been isolated from H_2O/TFE-d_3 solution by freeze-drying, in D_2O/TFE-d_3. Figure 9 shows the amide region of the NMR spectra of peptide LL9 at 1, 5, and 12 h after redissolving the peptide in 50% TFE-d_3 and 50% D_2O containing 0.1 M KCl, 50 mM PO_4, pH 5.2 The amide protons at the C- and N-terminals of the peptide exchange faster than other amide protons. The amide proton resonances of Glu-1, Glu-3, Lys-4, Glu-17, and the C-terminal amide disappear within 1 h. The results for Leu-2 and Lys-18 are ambiguous due to the overlap of their amide proton resonances with others (Figure 9). It is interesting to note that the amide protons of Leu-13, Leu-9, Leu-6, Leu-12, and Glu-10 exchange very slowly. Their proton resonances remain after 12 h (Figure 9D), indicating that these amides are involved in strong hydrogen bonds

(46) Eisenberg, D.; Weiss, R. M.; Terwilliger, T. C. *Nature* **1982**, *299*, 371–374.
(47) Eisenberg, D.; Schwarz, E.; Komaromy, M.; Wall, R. *J. Mol. Biol.* **1984**, *179*, 125–142.
(48) Gooley, P. R.; MacKenzie, N. E. *Biochemistry* **1988**, *27*, 4032–4040.
(49) Dempsey, C. E. *Biochemistry* **1986**, *25*, 3901–3911.

and/or that these amide protons are in a hydrophobic environment excluded from solvent molecules. Verification that the chemical shift (7.98 ppm) remaining after 12 h of hydrogen-deuterium exchange (Figure 9D) belongs to the Leu-12 amide rather than the Glu-15 amide was obtained by a HOHAHA 2D-NMR spectrum recorded between 7 and 12 h after the peptide was dissolved in D_2O/TFE-d_3. Recently, Ciesla et al.[50] observed a similar amide-exchange effect on a peptide which formed a four-helix bundle. They found that the hydrogen-deuterium exchange rate of the amide proton was decreased as the amide position was changed from end to central positions of the peptide, and these results can be explained if intermolecular association protects the amide protons from deuterium in the solvent.[48] However, the difference in exchange rates of different amides from this study cannot be explained by secondary structural differences or by intermolecular association, because it has been clearly demonstrated that the peptide LL9 is highly α-helical (CD and NMR studies) and is monomeric in 50% TFE (size-exclusion chromatography) and that the ellipticities at 220 nm are independent of peptide concentration (0.038-4.9 mM), suggesting no intermolecular association in 50% TFE.[29,35,51] The most plausible explanation is that this helical peptide has a time-averaged curvature with the hydrophobic face being concave, which results in the hydrophobic side chains in the center of hydrophobic face forming a hydrophobic microenvironment which protects the amide in this region from deuterium exchange with solvent molecules. The slow-exchange amides (Leu-13, Leu-9, Leu-6, Leu-12, and Glu-10) are all located in the center of hydrophobic face (Figure 6).

(50) Ciesla, D. J.; Gilbert, D. E.; Feigan, J. *J. Am. Chem. Soc.* **1991**, *113*, 3957-3961.
(51) Lyu, P. C.; Liff, M. I.; Marky, L. A.; Kallenbach, N. R. *Science* **1990**, *250*, 669-673.

Conclusions

This study has provided new insights into the relationship between amide chemical shifts and α-helical structure and demonstrated that the change in the amide chemical shift in an α-helix is not caused by the α-helical structure itself but is due to the amphipathic nature of the α-helix. These results suggest that the amide proton chemical shift is related to hydrogen-bond length and that a single-stranded amphipathic α-helix in solution is curved and this curved structure causes the upfield shifts of the amide protons in the convex side and the downfield shifts of the amide protons in the concave side. Understanding the relationship between the amide chemical shift and hydrogen-bond distance in an α-helical structure will have major implications in the studies of protein folding, protein-ligand binding, and protein-protein interactions, if these processes involve hydrogen bonds.

Acknowledgment. This project is an integral part of the Protein Engineering Network of Centres of Excellence Program supported by the Government of Canada. A postdoctoral fellowship stipend (N.E.Z.) and research allowance were provided by the Alberta Heritage Foundation for Medical Research. We thank Paul D. Semchuk and David Clarke for their assistance in peptide synthesis and purification and Bob Luty and Linda Golden for their skilled technical assistance in performing circular dichroism and NMR measurements.

^{13}C-$\{^1H\}$ NMR/NOE and Multiplet Relaxation Data in Modeling Protein Dynamics of a Collagen ^{13}C-Enriched Glycine GXX Repeat Motif Hexadecapeptide[‡,†]

Vladimir A. Daragan[§] and Kevin H. Mayo*

Contribution from the Structural Biology Group, Department of Pharmacology, The Jefferson Cancer Institute, Thomas Jefferson University, Philadelphia, Pennsylvania 19107.
Received August 15, 1991

Abstract: ^{13}C-NMR (75 MHz) multiplet spin-lattice (T_1) relaxation and ^{13}C-$\{^1H\}$ nuclear Overhauser measurements have been performed on a ^{13}C-glycine-XX repeating hexadecapeptide, i.e., GVKGDKGNPGWPGAPY, from the triple helix domain of collagen type IV. The data have been analyzed using a formalism that considers both autocorrelation and cross-correlation dipolar spectral densities. Several motional models were tested for consistency with the data. The terminal glycine, G1, and nonterminal glycines, G4, G7, G10, and G13, were found to have distinctly different motional properties that could not be explained simultaneously by any one model. Results indicate that most glycines rotate more isotropically than the N-terminal glycine. Analysis of the experimental data using several rotational models indicates that internal motions in the peptide are important to terminal, as well as nonterminal, ^{13}C-glycine relaxation. The character of the rotational motion of nonterminal glycines varies considerably with temperature. Although simple rotational diffusion models can describe terminal glycine motion, consideration of multiple internal rotations are necessary to fully describe nonterminal glycine rotations.

Introduction

Over the last 10 or so years, the functional significance of protein structural dynamics/internal motions in biological activity has been recognized. As a consequence, considerable effort has gone into characterizing protein/peptide side-chain and backbone motions, principally through temperature-dependent X-ray diffraction, NMR relaxation and amide exchange studies, and molecular dynamics simulations. NMR relaxation, in particular, is sensitive to a broad range of time scales. While measurement of most commonly used proton relaxation data can be acquired with rather good accuracy, the interpretation of such experimental data is complicated by the presence of multiple interproton motional vectors which are involved in deriving spectral densities.[1] An additional, nontrivial problem in interpreting these data lies in fully describing peptide bond rotations through the choice of an appropriate motional model. Numerous parameters are nec-

[‡]This work was made possible by a National Research Council/National Science Foundation International (U.S.S.R.) Project Development Grant to K.H.M. and benefitted from NMR facilities made available through Grant RR-04040 from the National Institutes of Health.
[†]Abbreviations: NMR, nuclear magnetic resonance; 2D-NMR, two-dimensional NMR spectroscopy; COSY, correlated spectroscopy; NOESY, nuclear Overhauser effect spectroscopy; NOE, nuclear Overhauser effect; rf, radio frequency; FID, free induction decay; IV-H1, parent peptide GVKGDKGNPGWPGAPY from type IV collagen; T_1, spin-lattice relaxation time; T_1(i), T_1 of ^{13}C-multiplet inner line (no proton decoupling); T_1(o), T_1 of ^{13}C-multiplet outer line (no proton decoupling); T_1, T_1 with proton decoupling.
[§]On leave from the Institute of Chemical Physics, Academy of Sciences of the USSR, 117977 Moscow, USSR.

(1) Torda, A. E.; Norton, R. S. *Biopolymers* **1989**, *28*, 703-716.

0002-7863/92/1514-4326$03.00/0